https://doi.org/10.5194/egusphere-2026-6297
Preprint. Discussion started: 17 November 2026
© Author(s) 2026. CC BY 4.0 License.

Detecting irrigation events by integrating multitemporal soil moisture dynamics and water-balance constraints

Shauifeng Peng[a], Jie Bai[a], Minghui Chang[a], Jiayu Zhu[a], Guangcheng Shao[b], Linguang Miao[c], Jinrui Fan[d], Shihua Li[a,e]*

[a] *School of Resources and Environment, University of Electronic Science and Technology of China, Chengdu 611731, China.*

[b] *College of Agricultural Science and Engineering, Hohai University, Nanjing 210098, China.*

[c] *School of Remote Sensing and Information Engineering, Wuhan University, Wuhan 430079, China*

[d] *College of Geography and Planning, Chengdu University of Technology, Chengdu 610059, China*

[e] *Technology Innovation Center for Southwest Land Space Ecological Restoration and Comprehensive Renovation, Ministry of Natural Resources, Chengdu, People's Republic of China*

**Address correspondence to: lishihua@uestc.edu.cn (S. Li)*

Abstract

Accurate monitoring of irrigation information is essential for sustainable agricultural water management. However, existing studies have focused on mapping irrigated areas and quantifying irrigation water use, while the timing of irrigation events remains insufficiently characterized. Soil moisture responds directly to irrigation, but rainfall produce similar signals, and response magnitude and duration vary among different irrigation events, making it severely challenging to differentiate

https://doi.org/10.5194/egusphere-2026-6297
Preprint. Discussion started: 17 November 2026
© Author(s) 2026. CC BY 4.0 License.

irrigation events. To this end, this study developed a novel framework irrigation events detection integrating multitemporal soil moisture dynamics and soil water balance constrains. Multi-depth observations were integrated into unified metrics, and non-irrigation water variations were characterized by the water balance model, while multi-timescale wetting signals and water balance residual jointly identified potential irrigation responses for consolidation into irrigation events through water-source attribution and integration of adjacent responses. This framework achieved robust performance against 149 reference irrigation events at five sites in China, the United States, and Morocco, with mean Precision, Recall, and F1 scores of 0.8321, 0.8111, and 0.8148, respectively, while gaining site-level F1 scores ranging from 0.7097 to 0.9574. Under rainfall–irrigation overlap, 75% of events were identified. Ablation analyses showed that direct wetting signals and water-source attribution reduced false detections from non-irrigation responses, whereas water balance residual improved detection of weak responses. Irrigation events detectability declined as observation interval increases, with median F1 scores decreasing to 0.62 and 0.53 at 5- and 6-day intervals, respectively. This framework provides a methodological foundation for extracting irrigation timing from satellite soil moisture observations and supporting regional agricultural water use monitoring.

Keywords: Irrigation events; Soil water balance; Soil moisture;

1.Introduction

Irrigation is a major anthropogenic water input for alleviating crop water stress and sustains agricultural production, while also modifying evapotranspiration and land-surface energy exchange through changes in soil moisture conditions (Chawla et al., 2020; Muturi et al., 2025). Accurate characterization of the spatial extent, water consumption, and timing of irrigation is therefore fundamental to assessing agricultural water use and its resulting hydrological impacts (Xiang et al., 2025). Existing studies have made substantial progress in identifying irrigated areas and quantifying irrigation water use across a range of spatial scales, whereas the timing of individual irrigation events and their temporal patterns remain comparatively underexplored (Le Page et al., 2023). Even under the same total irrigation amount, differences in irrigation frequency and event timing can lead to distinct soil moisture dynamics and subsequent hydrological responses. Consequently, Irrigation

https://doi.org/10.5194/egusphere-2026-6297
Preprint. Discussion started: 17 November 2026
© Author(s) 2026. CC BY 4.0 License.

event timing represents an important dimension of field-scale water management and provides critical temporal constraints for analyzing agricultural water consumption, interpreting evapotranspiration dynamics, and monitoring irrigation using remote sensing (Jalilvand et al., 2026).

Multi-source remote sensing time-series observations provide complementary avenues for retrieving irrigation timing information. However, different related remote sensing variables capture distinct land-surface responses to irrigation, which differ in both response latency and persistence. Vegetation indices primarily reflect the cumulative effects of irrigation on crop growth (Chen et al., 2018), whereas land surface temperature and evapotranspiration characterize irrigation-induced surface cooling and changes in surface energy partitioning (Jalilvand et al., 2026). In contrast, soil moisture responds more directly to water entering the soil, thereby providing an observational basis that is more closely linked to the irrigation process itself. Building on this characteristic, previous studies have identified potential irrigation events from increases in soil moisture between consecutive observations and have incorporated precipitation records or concurrent soil moisture changes in surrounding non-irrigated areas to reduce confusion with rainfall-induced wetting (Bazzi et al., 2020; Zappa et al., 2022). Bayesian change-point analysis has also been used to detect abrupt increases in soil moisture time series, providing structural evidence for temporally locating irrigation events (Gao et al., 2024). Nevertheless, soil moisture wetting is not uniquely indicative of irrigation, as rainfall can produce similar wetting responses. Moreover, the response magnitude and persistence of the post-irrigation soil moisture are influenced by antecedent soil moisture conditions, soil water infiltration and redistribution processes, as well as observation depth.

Water-balance approaches further constrain irrigation events detection from the perspective of water-budget accounting, either by inversely potential irrigation inputs or by identifying anomalous water inputs through comparisons between observed soil moisture changes and the changes expected under non-irrigated conditions (Brocca et al., 2018; Zappa et al., 2024). Their performance, however, depends in part on how reasonably background moisture dynamics are represented. Process-based simulations that explicitly describe evapotranspiration, drainage, and crop water use typically require a wide range of meteorological, vegetation, and soil parameters, and the associated parameterization and forcing data requirements make it more difficult to ensure data consistency and reliable availability across sites and over long time periods (Pereira et al., 2020; Le Page et al.,

https://doi.org/10.5194/egusphere-2026-6297
Preprint. Discussion started: 17 November 2026
© Author(s) 2026. CC BY 4.0 License.

2020). Meanwhile, when both irrigation timing and irrigation amount are unknown, the observed soil moisture series itself may contain the additional water inputs that are to be detected. If all observed variations are directly used to estimate model parameters, irrigation-induced wetting anomalies may bias parameter estimation, causing part of the irrigation signal to be absorbed into the baseline dynamics represented by the model. For studies aimed at detecting irrigation events rather than complete reconstruction of hydrological fluxes, it is therefore necessary to investigate how a background reference can be established from limited observations while reducing the influence of anomalous water inputs on parameter estimation without prespecifying irrigation dates to be specified a priori.

However, no single line of evidence corresponds uniquely to irrigation events. Rainfall can produce wetting responses similar to those induced by irrigation, while water-balance residuals may also be influenced by precipitation errors, biases in the background model, and hydrological processes that were not explicitly represented (Bazzi et al., 2020). Meanwhile, the magnitude and temporal structure of irrigation-induced soil moisture responses vary with irrigation practice, antecedent moisture conditions, and observation depth, ranging from abrupt increases to gradual wetting that persists for several days (Le Page et al., 2020; Le Page et al., 2023). A single irrigation event may generate multiple consecutive anomalous responses, whereas closely spaced irrigation events and concurrent rainfall may produce overlapping wetting processes. Consequently, soil-moisture-based irrigation event detection still requires methods that can accommodate diverse response patterns and observation conditions, distinguish anomalous moisture inputs from natural hydrological variability such as rainfall, and establish a robust temporal correspondence between continuous soil moisture responses and discrete irrigation events.

Beyond the non-uniqueness of moisture responses, limited temporal resolution further constrains the correspondence between observed soil moisture dynamics and individual irrigation events (Ozdogan et al., 2010). Existing soil moisture products still struggle to simultaneously meet the requirements of field-scale irrigation event monitoring for fine spatial resolution and temporal continuity (Zappa et al., 2022). As the observation interval increases, short-lived post-irrigation wetting peaks may occur between consecutive observations and partially dissipate before the next measurement, while rainfall and closely spaced irrigation events may fall within the same

https://doi.org/10.5194/egusphere-2026-6297
Preprint. Discussion started: 17 November 2026
© Author(s) 2026. CC BY 4.0 License.

observation interval (Gao et al., 2024). Consequently, distinct water inputs processes may be represented only by the net change between two observation endpoints (Zappa et al., 2022). Such loss of temporal information can not only lead to missed events but also increase the difficulty of distinguishing water sources and separating individual events. High-frequency in situ soil moisture measurements can more completely capturing the post-irrigation wetting and subsequent recession processes, provide a process-level reference for examining the temporal response of irrigation and evaluating the extent to which such responses are preserved under different observation frequencies.

Building on these considerations, this study developed an irrigation event detection framework that integrates multi-timescale soil moisture dynamics with a simplified soil water balance constraint. Specifically, the study aimed to: (1) evaluate the performance and differences of the framework for irrigation event detection across different sites; (2) characterize differences in irrigation event detectability under different soil moisture response patterns and irrigation conditions, and identify the major factors limiting detection; and (3) quantify the sensitivity of detection results to key parameter settings and assess irrigation event detectability under different soil moisture observation frequencies. This study is expected to improve understanding of the correspondence between soil moisture responses and irrigation events, while providing a methodological foundation for extending event-scale irrigation monitoring to regional agricultural hydrology and water resources research.

2.Materials and methods

2.1 Study area and in situ measurements

This study selected five agricultural field observation sites located across three major agricultural regions in China, the United States, and Morocco, namely Daman, US-Ne1, US-Ne2, F1, and F2 (Fig. 1). These sites encompass maize, soybean, and winter wheat cropping systems and represent diverse hydroclimatic conditions, irrigation management practices, and soil moisture observation configurations, providing a basis for evaluating the performance of irrigation event detection under heterogeneous conditions (Table 1). All sites are equipped with soil moisture measurements at multiple depths, together with corresponding irrigation records and precipitation

https://doi.org/10.5194/egusphere-2026-6297
Preprint. Discussion started: 17 November 2026
© Author(s) 2026. CC BY 4.0 License.

observations, providing the observational basis for irrigation event detection and performance evaluation.

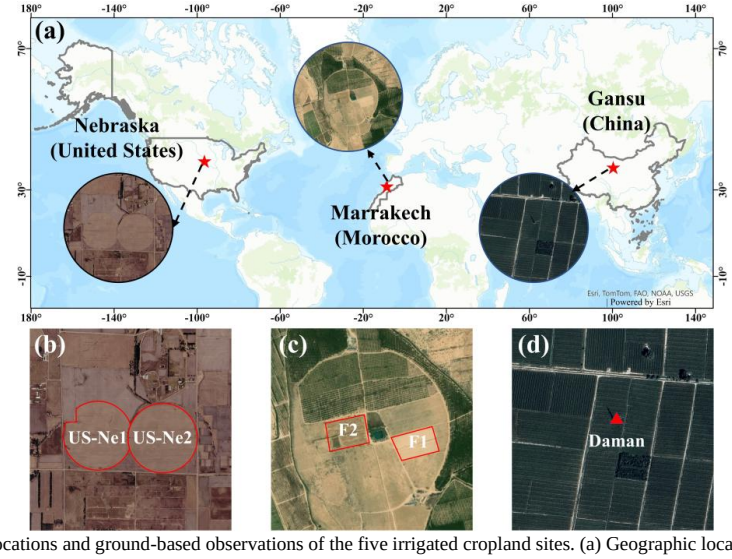


Fig. 1. Locations and ground-based observations of the five irrigated cropland sites. (a) Geographic locations of the study regions in Gansu, China; Nebraska, United States; and Marrakech, Morocco; (b) US-Ne1 and US-Ne2; (c) F1 and F2; (d) Daman.

The Daman site is located in the Daman Irrigation District of Zhangye City, Gansu Province, China. During the study period, maize was the dominant crop, and flood irrigation was the primary irrigation practice. The region is characterized by a temperate continental arid climate, with a long-term mean annual precipitation of approximately 130 mm and a mean annual potential evaporation of about 2002 mm. Natural precipitation is insufficient to meet crop water requirements, resulting in a strong dependence of agricultural production on irrigation (Liu et al., 2017; Liu et al., 2018; Liu et al., 2020; Liu et al., 2021; Liu et al., 2022; Liu et al., 2023; Liu et al., 2024; Liu et al., 2015).

The US-Ne1 and US-Ne2 sites are located within a long-term agricultural ecosystem observation area near Mead, Nebraska, United States. Both sites use center pivot irrigation, with continuous maize cultivation at US-Ne1 and a maize–soybean rotation at US-Ne2. The two sites share a humid continental climate, with a long-term mean annual precipitation of approximately 790 mm and a mean annual reference evapotranspiration of about 1415 mm. Irrigation therefore remains an important supplemental water source for maintaining crop water requirements (Andy Suyker 2026a; Andy Suyker 2026b).

https://doi.org/10.5194/egusphere-2026-6297
Preprint. Discussion started: 17 November 2026
© Author(s) 2026. CC BY 4.0 License.

The F1 and F2 sites are located on a private farm in Chichaoua Province on the Haouz Plain of central Morocco, approximately 65 km west of Marrakech. Both fields are cultivated with winter wheat under drip irrigation. The study area has a semi-arid Mediterranean climate, with a long-term mean annual precipitation of approximately 250 mm. Precipitation is concentrated mainly between October and April, whereas May to September constitutes the dry season. The long-term mean annual reference evapotranspiration is approximately 1600 mm, resulting in a pronounced climatic water deficit (Ouaadi et al., 2021).

Although the five sites differ in sensor installation depths and configurations, all provide continuous multi-depth soil moisture observations, precipitation records, and irrigation records suitable for irrigation event validation. To harmonize the temporal resolution across sites and match the daily temporal precision of the irrigation records, all original observations were aggregated to a daily time step. Daily soil water content was calculated as the arithmetic mean of all valid observations within each day, whereas precipitation was accumulated over the corresponding day. Missing periods were not filled by interpolation across calendar days.

Table 1. Characteristics of the five irrigated agricultural sites and datasets used in this study

Site	Location	Climate zone	Crop type	Irrigation method	Study period	Soil-moisture sensor depths (cm)	irrigation events (n)	Data access
Daman	38.8555° N, 100.3722° E	Temperate continental arid climate	Maize	Flood and drip irrigation	2016–2024 (2018 excluded)	2, 4, 10, 20, 40	47	https://data.tpdc.ac.cn
US-Ne1	41.1651° N, 96.4766° W	Humid continental climate	Maize	Center-pivot irrigation	2014–2021 (2019 excluded	10, 25, 50	35	10.17190/AMF/1246084
US-Ne2	41.1649° N, 96.4701° W	Humid continental climate	Maize–soybean rotation	Center-pivot irrigation	2014–2021	10, 25, 50	31	10.17190/AMF/1246085
F1	31.4269° N, 8.6499° W	Semi-arid Mediterranean climate	Winter wheat	Drip irrigation	Dec 2016–Jul 2018	5, 25, 35	14	10.23708/8D6WQC
F2	31.4273° N, 8.6532° W	Semi-arid Mediterranean climate	Winter wheat	Drip irrigation	Dec 2016–Jul 2018	5, 30	22	10.23708/8D6WQC

Note: The Daman site was irrigated by flood irrigation in 2016, switched to drip irrigation during 2017–2018, and returned to flood irrigation from 2019 to 2024.

2.2 Overall methodology

The proposed framework uses daily soil moisture and precipitation time series as inputs to establish a cross-site irrigation event detection framework (Fig. 2). First, soil moisture observations at different depths across sites are harmonized into mean volumetric soil water content over 0–10 cm and soil water storage over 0–30 cm. A simplified soil water balance model was then established

https://doi.org/10.5194/egusphere-2026-6297
Preprint. Discussion started: 17 November 2026
© Author(s) 2026. CC BY 4.0 License.

using rainfall, antecedent water storage, and seasonal variability to estimate background changes in soil water storage. A robust iterative fitting procedure is employed to reduce the influence of potential anomalous water inputs on model estimation. The difference between the observed and background-estimated changes in soil water storage is defined as the water balance residual. Direct wetting responses, together with cumulative water balance residuals at multiple temporal scales, are subsequently used to identify candidate irrigation responses. These candidates are further subjected to water-source attribution using recent rainfall, rainfall-adjusted in storage changes, and water balance residuals, while Auxiliary depth responses provide additional evidence for boundary candidates with insufficient supporting evidence. Finally, temporal localization and event consolidation are applied to convert continuous anomalous responses into discrete irrigation events. The detected events are then evaluated through event-level one-to-one matching against reference irrigation records, enabling quantitative assessment of irrigation event detection performance.

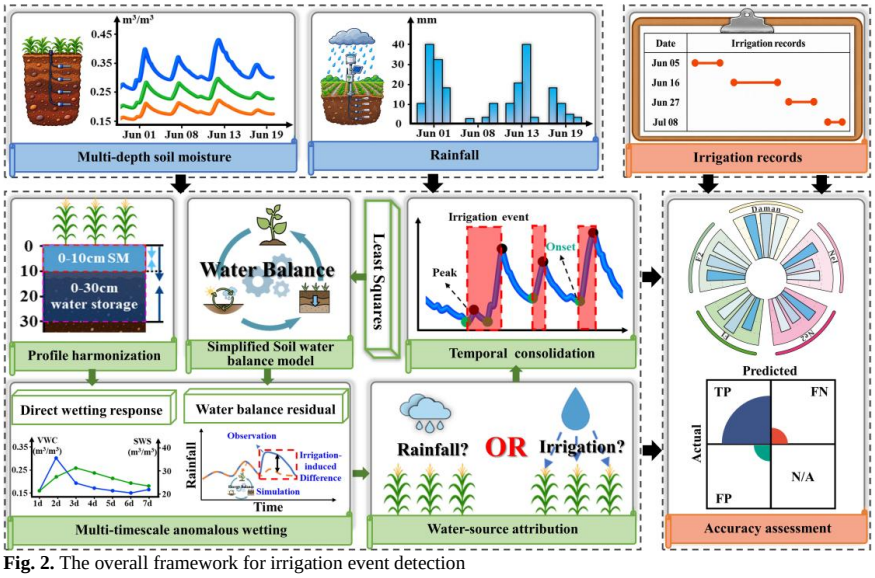


Fig. 2. The overall framework for irrigation event detection

2.3 Harmonization of soil moisture profiles

Soil moisture sensors differed among sites in both measurement depth and vertical configuration, such that direct cross-site comparisons based on individual sensor records could confound actual soil moisture responses with differences arising from measurement depth (Babaeian et al., 2019). To derive analysis variables representing consistent target soil layers across sites, the

https://doi.org/10.5194/egusphere-2026-6297
Preprint. Discussion started: 17 November 2026
© Author(s) 2026. CC BY 4.0 License.

multi-depth soil moisture observations were harmonized into mean volumetric soil water content over 0–10 cm and soil water storage over 0–30 cm. The 0–10 cm mean volumetric soil water content was used to characterize the rapid wetting response of shallow soil following irrigation or rainfall, whereas the 0–30 cm soil water storage was used to represent integrated changes in water content across the near-surface soil profile.

For each observation day, the soil moisture profile was reconstructed using piecewise linear interpolation between adjacent depths with valid measurements. For the unobserved soil layer between the surface and the shallowest measurement depth, volumetric soil water content was assumed to be equal to the observed value at the shallowest depth. When no direct measurement was available at 30 cm, the volumetric soil water content at 30 cm was estimated by linear interpolation between the nearest valid measurements above and below this depth (Amankwah et al., 2022). Profile reconstruction relied exclusively on valid observations from the same day, with no interpolation performed in the temporal dimension. $\tilde{\theta}(z,t)$ denote the reconstructed volumetric soil water content at depth (z) on day (t). The 0–30 cm soil water storage and the 0–10 cm mean volumetric soil water content were then expressed as:

$$S_t = 10\int_0^{30}\tilde{\theta}(z,t)\mathrm{d}z \quad (1)$$

$$\bar{\theta}_t = \frac{1}{10}\int_0^{10}\tilde{\theta}(z,t)\mathrm{d}z \quad (2)$$

Where S_t denotes soil water storage in the 0–30 cm (mm), and $\bar{\theta}_t$ denotes mean volumetric soil water content in the 0–10 cm ($m^3\ m^{-3}$). The integrals were evaluated numerically using the trapezoidal rule.

2.4 Robust estimation of background soil water storage changes

Changes in soil water storage are jointly influenced by rainfall inputs, soil moisture recession, and additional water inputs such as irrigation. When irrigation inputs are unknown, directly fitting the model to all observed changes may allow irrigation-induced wetting anomalies to influence the estimation of model parameters (Zappa et al., 2020). To reduce the dependence of irrigation event detection on externally specified parameters, a simplified soil water balance representation was

https://doi.org/10.5194/egusphere-2026-6297
Preprint. Discussion started: 17 November 2026
© Author(s) 2026. CC BY 4.0 License.

adopted. The model describes water inputs using the immediate and lagged contributions of rainfall, while the combined effects of processes such as evapotranspiration and drainage are represented by antecedent soil water storage and seasonal variability, without independently resolving individual loss fluxes (Pereira et al., 2020). The model was used to approximate the expected daily change in 0–30 cm soil water storage under a no-irrigation baseline, expressed as:

$$\widehat{\Delta S}_t^0 = \sum_{k=0}^{2} c_k P_{t-k} - a_0 \exp[a_1 \sin(\omega\tau_t) + a_2 \cos(\omega\tau_t)]\, x_{t-1}^b \quad (3)$$

where the first term represents the immediate and lagged effects of rainfall over the current day and the preceding 2 days on soil water storage in the 0–30 cm layer. P_{t-k} denotes rainfall on day *t-k*, and c_k represents the contribution of rainfall at a lag of *k* days to the change in soil water storage. The second term jointly accounts for soil water depletion associated with processes such as evapotranspiration and drainage as a function of antecedent storage conditions and seasonal variability. The parameter a_0 controls the baseline magnitude of soil water depletion, *b* describes its nonlinear dependence on soil water storage, and a_1 and a_2 characterize intra-annual seasonal variability. Here, $\omega = 2\pi/365.25$, τ_t denotes the temporal position within the annual cycle, and x_{t-1} is the normalized soil water storage state on the preceding day. For each site, x_{t-1} was normalized to the range 0–1 using the 1st and 99th percentiles of soil water storage as the lower and upper normalization bounds, respectively.

To ensure physically plausible parameter ranges and prevent negative contributions from rainfall or negative soil water depletion, the following constraints were imposed during parameter estimation:

$$c_k \geq 0, \quad \sum_{k=0}^{2} c_k < 1,$$
$$0 < a_0 \leq 100, \quad -3 \leq a_1, \quad a_2 \leq 3, \quad 0.5 \leq b \leq 4 \quad (4)$$

Meanwhile, the observed soil moisture time series may contain unknown irrigation inputs or other anomalous. Directly estimating model parameters from all observed changes could therefore allow anomalous wetting to influence the background dynamics. Model parameters were estimated separately for each site without using the reference irrigation records to prespecify calibration dates. First, the model parameters were estimated from valid observation dates using bounded nonlinear least squares with a soft-L1 robust loss function to reduce the influence of large residuals on

https://doi.org/10.5194/egusphere-2026-6297
Preprint. Discussion started: 17 November 2026
© Author(s) 2026. CC BY 4.0 License.

parameter estimation (Virtanen et al., 2020). Anomalously positive residuals were then identified from the differences between observed and background-predicted changes in soil water storage, and the corresponding dates were excluded from the subsequent parameter estimation. This procedure was repeated until the stopping criterion was met or the maximum number of iterations was reached. For date *t*, the water-balance residual was defined as:

$$e_t = \Delta S_t - \widehat{\Delta S}_t^0 \quad (5)$$

where e_t denotes the water-balance residual on day *t* (mm d^{-1}); ΔS_t represents the observed daily change in soil water storage over 0–30 cm; and $\widehat{\Delta S}_t^0$ represents the expected daily change in soil water storage under the no-irrigation baseline.

Because the variability of water-balance residuals differs among sites, a robust median–MAD standardization was applied to transform the residuals into a comparable dimensionless anomaly scale across sites:

$$Z_{I,t} = \frac{e_t - median(e_I)}{1.4826 MAD(e_I)} \quad (6)$$

Where $Z_{I,t}$ denotes the standardized water-balance residual on day *t*; *I* is the set of calibration samples retained after convergence of the iterative procedure; e_I denotes the water-balance residual for sample *I*; and MAD is the median absolute deviation of the residuals from their median. The factor 1.4826 scales the MAD to a robust dispersion estimate comparable to the standard deviation (Rousseeuw and Croux 1993).

2.5 Multi-timescale detection of wetting anomalies

Soil moisture responses to irrigation inputs may manifest as either rapid wetting over a short period or gradual changes persisting for several days, depending on infiltration dynamics, irrigation duration, and observation depth. To accommodate soil moisture responses with different durations, this study constructed multi-timescale wetting anomaly indicators from two complementary perspectives: direct wetting responses and water-balance deviations from the no-irrigation baseline. These indicators were subsequently used to identify potential irrigation events.

For the direct wetting response, changes in 0–30 cm soil water storage and mean volumetric soil water content in the 0–10 cm layer were calculated relative to observations 1, 2, 3, 5, and 7 days earlier. Each change metric was robustly standardized using the median–MAD formulation in Eq.

https://doi.org/10.5194/egusphere-2026-6297
Preprint. Discussion started: 17 November 2026
© Author(s) 2026. CC BY 4.0 License.

(6), and the maximum standardized response across all variables and temporal scales was denoted as M_t, representing the most pronounced direct wetting anomaly on day *t*. The use of multiple temporal scales allows both rapid wetting and wetting responses manifested over several days to be captured, thereby reducing the dependence of irrigation event detection on any single response timescale.

For the water-balance deviation from the no-irrigation baseline, water-balance residuals were accumulated over consecutive 1-, 3-, 5-, and 7-day windows to characterize the cumulative deviation of observed soil water storage changes from the no-irrigation baseline prediction across different temporal scales. Each accumulated residual was likewise robustly standardized using the median–MAD formulation in Eq. (6), and the maximum standardized anomaly across the different windows was denoted as C_t, representing the magnitude of persistent anomalous water-balance deviation.

The larger of the direct wetting anomaly M_t and the accumulated water-balance residual anomaly C_t was defined as the integrated wetting anomaly indicator:

$$E_t = \max(M_t, C_t) \quad (7)$$

Within continuous sequences of valid E_t, local peaks were identified based on the integrated candidate peak threshold, and a minimum separation between candidate peaks was imposed to reduce duplicate detection of the same persistent wetting process. To avoid generating candidates solely from standardized anomalies or deviations in background predictions, candidate dates were additionally required to show an actual increase in soil water storage at least at one of the analysis timescales. The candidates were then further screened by considering soil water storage recession state represented by the no-irrigation baseline and the preceding changes in soil water storage, retaining wetting responses that showed a clear deviation from the background dynamics and were associated with a plausible antecedent moisture state. Definitions, reference values, and sensitivity ranges of the key parameters for irrigation event detection are provided in Table 2.

Table 2. Definitions, baseline values, and sensitivity-analysis settings of the eight key parameters for irrigation event detection.

Parameter	Role	Baseline value	Values tested
Candidate peak	Sets the minimum integrated wetting anomaly E_t required for candidate selection.	3.0	2.0、2.5、3.0、3.5、4.0
Candidate Peak separation	Reduces adjacent candidate peaks arising from the same persistent wetting episode.	4 d	2、3、4、5、6 d

https://doi.org/10.5194/egusphere-2026-6297
Preprint. Discussion started: 17 November 2026
© Author(s) 2026. CC BY 4.0 License.

Background recession percentile	Screens candidates using the within-site percentile rank of the negative predicted background storage change.	0.35	0.25、0.30、0.35、0.40、0.45
Antecedent storage recession	Constrains storage changes preceding candidate wetting responses.	-1.0	−2.0、−1.5、−1.0、−0.5、0
Water-balance residual under rainfall–irrigation overlap	Constrains the water-balance residual anomaly of candidates under rainfall-irrigation overlap.	2.5	1.5、2.0、2.5、3.0、3.5
Rainfall-adjusted storage anomaly	Supports water-source attribution under rainfall jointly with the water-balance residual criterion.	2.0	1.0、1.5、2.0、2.5、3.0
Immediate storage response	Confirms a temporally identifiable one-day wetting response on the candidate date.	2.5	1.5、2.0、2.5、3.0、3.5
Event merge gap	Constrains the merging of adjacent responses together with storage persistence.	4 d	0、2、4、6、8 d

Note: Except for the temporal intervals and percentile thresholds, all thresholds are decision values defined for dimensionless indices.

2.6 Water-source attribution

The identified potential irrigation events require further water-source attribution. Accordingly, concurrent rainfall, water-balance residuals, and rainfall-adjusted changes in soil water storage were jointly examined to determine whether a potential event was supported by evidence of irrigation input, rather than directly attributing an isolated anomalous wetting signal to irrigation (Le Page et al., 2020).

First, to evaluate the relationship between observed changes in soil water storage and concurrent rainfall across different temporal scales, the difference between the change in 0–30 cm soil water storage and the corresponding accumulated rainfall was calculated for each storage-change window of length w:

$$R_{w,t} = (S_t - S_{t-w}) - \sum_{j=0}^{w+1} P_{t-j}, w \in \{1,2,3,5,7\} \quad (8)$$

where $R_{w,t}$ denotes the rainfall-adjusted change in soil water storage over a time window of length w. The precipitation accumulation period was extended by 2 days prior to the soil water storage change window to account for the lagged influence of rainfall on subsequent soil moisture responses. P_{t-j} denotes precipitation on day t-j and j represents the rainfall lag in days. The $R_{w,t}$ values at different temporal scales were robustly standardized using the same median–MAD formulation as in Eq. (6).

Based on the cumulative rainfall on the day of each potential irrigation event and the preceding 2 days, together with the anomaly magnitudes of the water-balance residual and the rainfall-adjusted soil water storage change, the water-source attribution rules were defined as follows:

https://doi.org/10.5194/egusphere-2026-6297
Preprint. Discussion started: 17 November 2026
© Author(s) 2026. CC BY 4.0 License.

$$\begin{cases} \text{Rain-free irrigation} & \sum_{j=0}^{2} P_{t-j} < 0.2, \\ \text{Rainfall-Irrigation overlap,} & \sum_{j=0}^{2} P_{t-j} \geq 0.2, \quad \max(Z_I) \geq 2.5, \quad \max(Z_R) \geq 2.0, \\ \text{Rainfall,} & \text{otherwise.} \end{cases} \tag{9}$$

where $\max(Z_I)$ denotes the maximum standardized water-balance residual within ±*1* day of the candidate event date, and $\max(Z_R)$ denotes the maximum standardized rainfall-adjusted soil water storage change across the 1, 2-, 3-, 5-, and 7-day windows.

For candidate events that could not be unambiguously classified using the primary water-source attribution criteria, soil moisture changes at auxiliary depths (10–30 cm) were further examined. The median soil water content during the 5 days preceding the candidate event was taken as the antecedent condition and compared with the maximum soil water content observed from the candidate day to 3 days afterward. The resulting wetting response was standardized using the MAD-based scale of daily soil moisture changes at the corresponding depth. A candidate event was considered to have supported evidence of wetting at auxiliary depths when the standardized wetting response reached or exceeded 1.0 at least one auxiliary depth. Auxiliary-depth information was used only for further discrimination of borderline events and was not imposed as a universal detection criterion for all potential irrigation events.

2.7 Irrigation event definition and temporal consolidation

Candidate events retained after water-source attribution were evaluated using an immediate storage response threshold based on the standardized one-day change in 0–30 cm soil water storage on the candidate date, to confirm the presence of a temporally identifiable wetting response. Because multi-timescale anomaly peaks may occur after the initial soil moisture wetting response, the confirmed candidate events were subsequently subjected to temporal localization. Starting from each candidate date, the preceding 2 days were examined backward based on changes in soil water storage, and the earliest date satisfying the start of response wetting criterion was identified as the response onset. If no earlier valid response was identified, the candidate date was retained as the response onset. To reduce duplicate detection of the same persistent wetting process, adjacent response onsets were further consolidated according to their temporal separation and the intervening

https://doi.org/10.5194/egusphere-2026-6297
Preprint. Discussion started: 17 November 2026
© Author(s) 2026. CC BY 4.0 License.

soil water storage state. Responses occurring on consecutive dates were directly merged. When a gap was present, responses were assigned to the same event only when the number of non-response days did not exceed the prescribed consolidation interval, observations were complete throughout the gap, and soil water storage remained above the pre-event background level. After consolidation, the earliest and latest response onsets within each group were used to define the temporal range of the detected event, and the response onset with the strongest anomalous signal was selected as the representative event date.

2.8 Accuracy assessment

Within each site, detected and reference irrigation events were matched using a global one-to-one matching procedure with a temporal tolerance of ±1 day. Each reference irrigation event was allowed to match at most one detected event to avoid duplicate counting. Successfully matched detected events were classified as true positives (TP), detected events without a corresponding reference event as false positives (FP), and reference events without a corresponding detected event as false negatives (FN). Event-level Precision, Recall, and F1 score were defined as:

$$\text{Precision} = \frac{TP}{TP + FP} \tag{10}$$

$$\text{Recall} = \frac{TP}{TP + FN} \tag{11}$$

$$\text{F1} = \frac{2 \times Precision \times \text{Recall}}{Precision + Recall} \tag{12}$$

3.Results

3.1 Irrigation events detection performance

The framework achieved consistently good performance across the five sites, with mean Precision, Recall, and F1 scores of 0.8321, 0.8111, and 0.8148, respectively (Fig. 3a). Of the 149 reference irrigation events, 120 were successfully matched, whereas 29 were missed. Among the 140 detected events, 20 were not matched to any reference irrigation record (Fig. 3b–f). Among these, Daman exhibited the highest and most balanced detection performance, with 45 of the 47 reference events correctly detected and identical Precision, Recall, and F1 scores of 0.9574. Sites of F1 and F2 showed moderately lower overall performance than Daman, with F1 scores of 0.8125 and 0.8444, respectively. Detection performance was lower at US-Ne1 and US-Ne2, where the F1

https://doi.org/10.5194/egusphere-2026-6297
Preprint. Discussion started: 17 November 2026
© Author(s) 2026. CC BY 4.0 License.

scores were 0.7097 and 0.7500, respectively. Despite this decrease, Precision remained above 0.815 at both sites. Together, US-Ne1 and US-Ne2 accounted for 23 missed events, representing 79.3% of all missed events across the five sites.

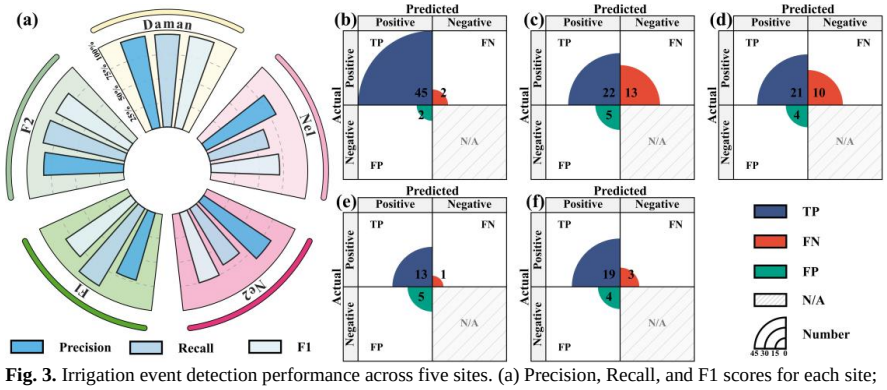


Fig. 3. Irrigation event detection performance across five sites. (a) Precision, Recall, and F1 scores for each site; (b–f) event-matching outcomes for Daman, US-Ne1, US-Ne2, F1, and F2, respectively.

3.2 Irrigation event detection under different rainfall conditions

The overall detection rate of reference irrigation events was higher under rain-free conditions than under rainfall–irrigation overlap. Of the 149 reference irrigation events, 49 occurred under rain-free conditions, of which 45 were correctly detected, accounting for 91.8%. The remaining 100 events overlapped with rainfall, of which 75 were correctly detected, accounting for 75.0%. These results indicate that the proposed framework was able to detect the majority of irrigation events even in the presence of rainfall. Among the 29 missed irrigation events, 25 occurred under rainfall–irrigation overlap, accounting for 86.2% (Fig. 4a), indicating that rainfall–irrigation overlap was a common characteristic of missed detections.

Besides, Fig. 4b further shows the irrigation event detection rates at each site under rain-free and rainfall–irrigation overlap conditions. Detection rates under rain-free conditions exceeded 80.0% at all five sites, reaching 95.0%, 90.0%, and 91.7% at Daman, F1, and F2, respectively. Because only a small number of rain-free irrigation events occurred at US-Ne1 and US-Ne2, their detection rates were not further compared. Under rainfall–irrigation overlap, inter-site differences in detection rate became more pronounced. US-Ne1 and US-Ne2 exhibited the lowest detection rates, at 60.0%

https://doi.org/10.5194/egusphere-2026-6297
Preprint. Discussion started: 17 November 2026
© Author(s) 2026. CC BY 4.0 License.

and 65.5%, respectively, whereas Daman maintained a high detection rate of 96.3%. These results suggest that although rainfall–irrigation overlap increased the difficulty of irrigation event detection at some sites, the proposed method was still able to detect most irrigation events across different rainfall conditions.

Fig. 4c further compares the distributions of 0–2-day cumulative rainfall associated with matched and missed irrigation events. For US-Ne1 and US-Ne2, where missed events were relatively frequent, it can be found the median cumulative rainfall associated with missed events was higher than that associated with matched events. However, the rainfall distributions of matched and missed events overlapped substantially, with no distinct rainfall threshold separating the two groups. This further suggests that the difficulty of irrigation event detection is related not only to the temporal overlap between rainfall and irrigation, but potentially also to the amount of concurrent rainfall. Nevertheless, rainfall amount alone does not determine whether an irrigation event can be detected; its influence is more likely governed by the extent to which irrigation-induced and rainfall-induced soil moisture responses can be distinguished.

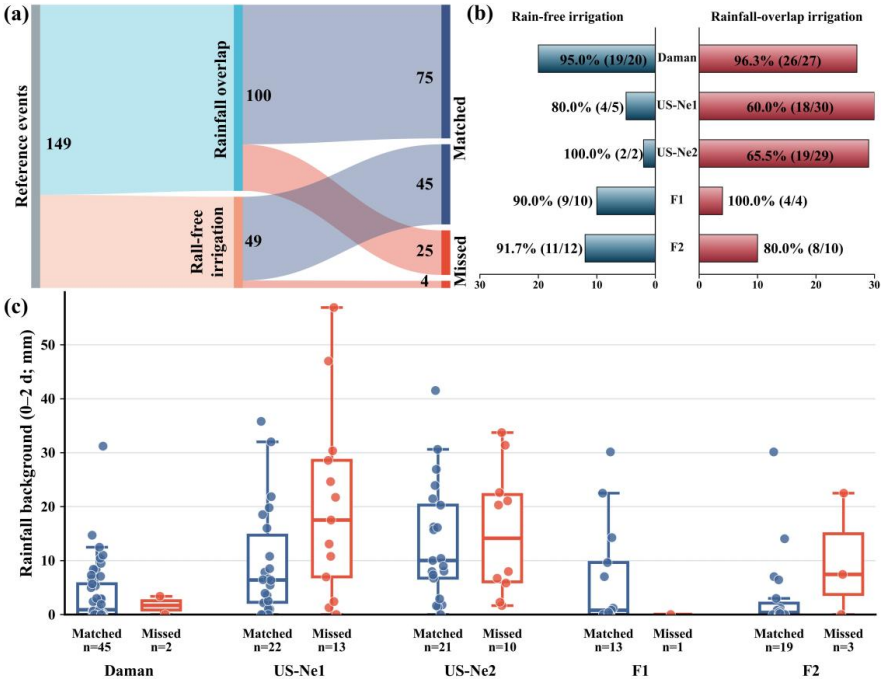


Fig. 4. Irrigation event detection under different rainfall conditions. (a) Detection outcomes of reference irrigation events under rain-free and rainfall–irrigation overlap; (b) irrigation event detection rates under rain-free and rainfall–

https://doi.org/10.5194/egusphere-2026-6297
Preprint. Discussion started: 17 November 2026
© Author(s) 2026. CC BY 4.0 License.

irrigation overlap across five sites; (c) distributions of 0–2-day cumulative rainfall associated with matched and missed irrigation events across five sites.

3.3 Contributions of different evidence components to irrigation events detection

To reveal the specific contributions of different evidence components to irrigation events detection, we conducted the ablation experiments, and results demonstrated that different evidence components played distinct constraining roles in irrigation event detection framework. Overall, direct soil moisture responses had the most pronounced influence on detection performance, while water-source attribution and soil water balance constraints also made substantial contributions. In contrast, auxiliary-depth responses had a comparatively limited effect (Fig. 5).

Removing the direct soil moisture response (A) reduced the mean Precision, Recall, and F1 score to 0.4686, 0.7433, and 0.5684, respectively (Fig. 5a), while increasing the number of FP events by 122 relatives to the full framework (Fig. 5b). F1 scores decreased at all five sites, with particularly pronounced reductions at US-Ne2, F1, and F2, where the decreases were 0.4252, 0.2720, and 0.2675, respectively (Fig. 5c). The direct soil moisture responses provide a fundamental observability constraint for irrigation event detection. They not only provide direct evidence of wetting associated with irrigation, but also contribute to the screening and confirmation of candidate events, thereby limiting the inclusion of anomalous candidates that lack clear support from a direct wetting response in the final event set.

Removing the soil water balance constraints (B) reduced the mean Precision, Recall, and F1 score to 0.6427, 0.7646, and 0.6929, respectively (Fig. 5a), while increasing the number of FP events by 45 relatives to the full framework (Fig. 5b). Sensitivity to this evidence component varied among sites, with relatively pronounced reductions in F1 at US-Ne2, US-Ne1, and F2 of 0.2269, 0.1580, and 0.1302, respectively (Fig. 5c). The soil water balance constraints provide complementary evidence to direct soil moisture responses by quantifying anomalous deviations of observed soil water storage changes from the expected dynamics under the no-irrigation baseline. It also imposes an additional constraint on candidate events that lack sufficient support from anomalous water-balance signals.

https://doi.org/10.5194/egusphere-2026-6297
Preprint. Discussion started: 17 November 2026
© Author(s) 2026. CC BY 4.0 License.

Removing water-source attribution (C) reduced the mean Precision and F1 score to 0.5582 and 0.6587, respectively, while increasing Recall to 0.8410 (Fig. 5a). Although 6 additional reference irrigation events were detected relative to the full framework, this gain was accompanied by 98 additional false-positive events (Fig. 5b). Precision decreased at all five sites, with the largest reduction observed at US-Ne2 (0.5842) (Fig. 5c). Water-source attribution provides an important constraint for distinguishing irrigation from other water-input processes. Without this constraint, more reference irrigation events can be retained, but at the cost of allowing a large number of anomalous candidates with ambiguous water sources to enter the final event set.

In contrast, auxiliary-depth responses (D) had a relatively limited influence on overall performance. Removing this evidence component resulted in near-zero performance changes at most sites. Although its contribution to overall performance was modest, auxiliary-depth responses information still provided additional vertical evidence of wetting for a subset of candidate events, serving as supplementary support for event determination.

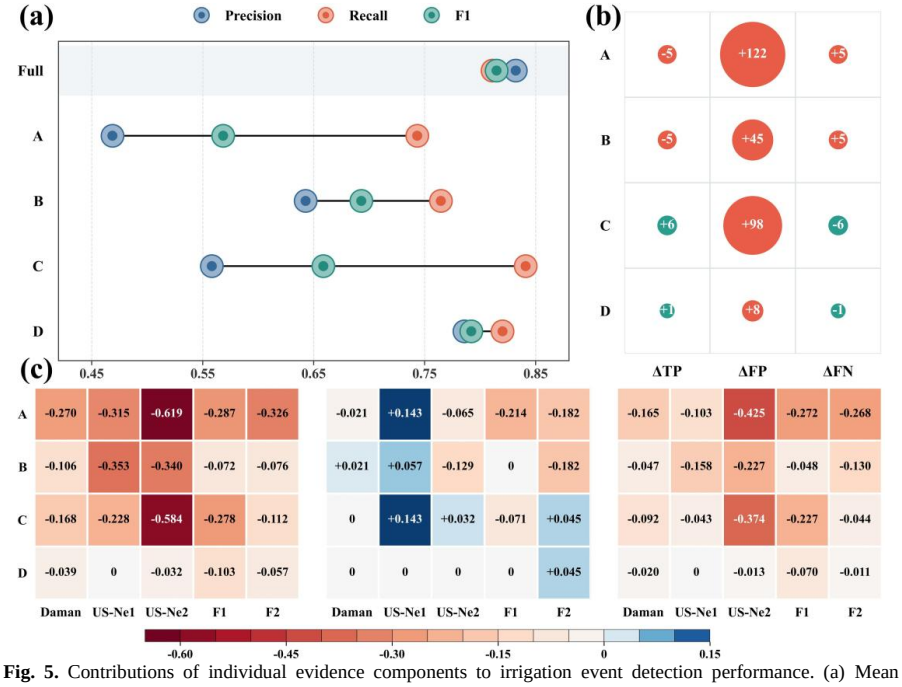


Fig. 5. Contributions of individual evidence components to irrigation event detection performance. (a) Mean Precision, Recall, and F1 score across the five sites for the full framework and the ablation scenarios in which direct soil moisture response (A), soil water balance constraints (B), water-source attribution (C), and auxiliary-depth response (D) were removed separately; (b) changes in TP, FP, and FN for each ablation scenario relative to the full

https://doi.org/10.5194/egusphere-2026-6297
Preprint. Discussion started: 17 November 2026
© Author(s) 2026. CC BY 4.0 License.

framework for ablation experiments; (c) changes in Precision, Recall, and F1 score at each site relative to the full framework for ablation experiments.

3.4 Major limiting factors for missed reference irrigation events

Event-by-event diagnosis of the 29 missed irrigation events indicated that the main limitations could be grouped into three categories. 11 events involved insufficient response evidence or pre-irrigation background conditions that did not satisfy the detection; another 11 involved temporal offsets between the detected response and the reference irrigation record or the consolidation of adjacent events; and the remaining 7 were primarily associated with ambiguous water-source attribution.

Fig. 6 illustrates three representative types of missed detections. In the US-Ne2 case, soil moisture at different depths showed only minor changes following irrigation and did not form a distinct response against the antecedent wet background (Fig. 6a). This example indicates that irrigation does not necessarily produce a clearly distinguishable soil moisture anomaly. When irrigation-induced changes are small or insufficiently distinct from the pre-irrigation background, soil moisture observations alone may provide insufficient evidence for irrigation detection. In the US-Ne1 case, a pronounced increase in soil moisture was observed, but the main response and the detected event were temporally offset from the reference irrigation date (Fig. 6b). This pattern more likely reflects a mismatch between the timing of the reference event and the actual soil moisture response rather than the absence of a wetting signal, although some uncertainty in the recorded irrigation timing cannot be ruled out. In the F2 case, rainfall and the reference irrigation event substantially overlapped in time (Fig. 6c). The increase in soil moisture also showed stronger temporal correspondence with the rainfall process, making the wetting response more readily attributable to rainfall and preventing the formation of independent evidence that could be clearly attributed to irrigation.

https://doi.org/10.5194/egusphere-2026-6297
Preprint. Discussion started: 17 November 2026
© Author(s) 2026. CC BY 4.0 License.

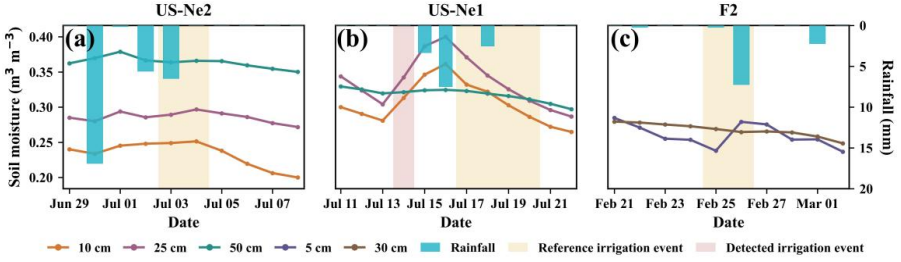


Fig. 6. Soil moisture and rainfall dynamics for representative missed reference irrigation events. (a) Insufficient response evidence or incompatible pre-irrigation background conditions; (b) temporal offset between the detected event and the reference irrigation timing; (c) ambiguous water-source attribution.

3.5 Effects of revisit interval on irrigation event detection

As the soil moisture revisit interval increased from 1 to 6 days, the mean Precision across the five sites remained above 0.70, whereas Recall declined from 0.81 to 0.45 and F1 from 0.81 to 0.53 (Fig. 7a). As the observation interval increased, irrigation, rainfall, and subsequent soil moisture recession were increasingly compressed into the net change between consecutive observations, thereby weakening information on irrigation event timing and the temporal correspondence their soil moisture responses.

The 5- and 6-day scenarios further highlighted the temporal sampling limitations associated with revisit intervals approaching the nominal revisit scales of Sentinel-2 and Sentinel-1, respectively. At a 5-day revisit interval, the mean Precision, Recall, and F1 score were 0.73, 0.55, and 0.62, respectively, compared with 0.71, 0.45, and 0.53 at a 6-day interval. Variability caused by different sampling start dates was smaller than the overall performance degradation associated with increasing revisit interval, indicating that the decline was not driven by a few unfavorable sampling schedules but primarily reflected the irrecoverable loss of temporal information within the observation gaps. For irrigation events with short response durations or limited response magnitudes, soil moisture increases may also be attenuated by evapotranspiration, drainage, and redistribution before the next observation, further reducing their detectability in sparsely sampled time series.

Sensitivity to temporal sparsification varied markedly among sites (Fig. 7b). Daman maintained relatively high F1 scores even under 5-6-day revisit intervals, whereas the F1 and F2 sites showed moderate declines and the US-Ne1 and US-Ne2 sites were generally more sensitive to

https://doi.org/10.5194/egusphere-2026-6297
Preprint. Discussion started: 17 November 2026
© Author(s) 2026. CC BY 4.0 License.

increasing revisit interval. These differences may be related to the separability of irrigation-induced responses from background soil moisture variability at each site. Under arid conditions, weaker rainfall interference and a higher contrast between irrigation-induced wetting and background soil moisture dynamics may help preserve the detectability of wetting signals over longer observation intervals. As natural wetting processes become more frequent, irrigation responses are more likely to overlap temporally with rainfall and background soil moisture variations, thereby increasing ambiguity in water-source attribution and the likelihood of missed irrigation events under sparse observations.

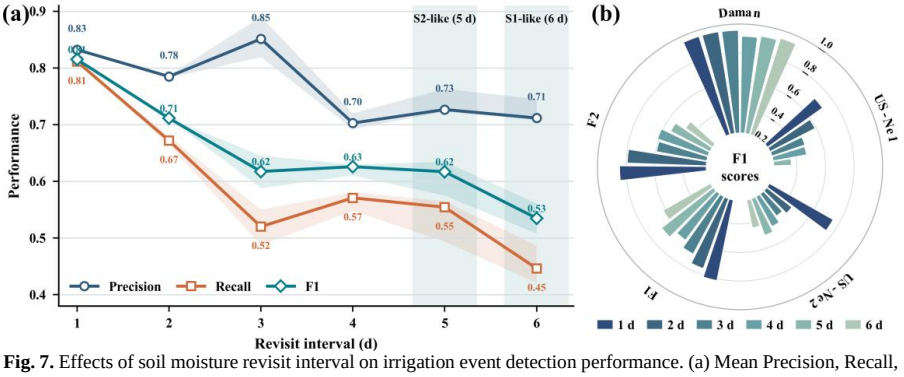


Fig. 7. Effects of soil moisture revisit interval on irrigation event detection performance. (a) Mean Precision, Recall, and F1 score across the five sites under revisit intervals of 1-6 days; (b) site-specific changes in F1 score across revisit intervals. Results were aggregated across different sampling start dates, and the shaded areas indicate the corresponding range of variation.

4. Discussion

4.1 Parameter Sensitivity Analysis

To assess the robustness of the irrigation events detection framework to parameter selection, we conducted a one-at-a-time sensitivity analysis by varying each of the eight key parameters across its tested range while holding the others at their baseline values. Sensitivity analysis showed that the candidate peak (Fig. 8a), antecedent storage recession (Fig. 8d), and water-balance residual under rainfall–irrigation overlap (Fig. 8e) caused little change in detection performance over the tested ranges. The changes in F1 score associated with the background recession percentile (Fig. 8c) and immediate storage response (Fig. 8g) were also both smaller than 1.84 percentage points. In

https://doi.org/10.5194/egusphere-2026-6297
Preprint. Discussion started: 17 November 2026
© Author(s) 2026. CC BY 4.0 License.

contrast, the consolidation interval between event merge gap (Fig. 8h), candidate peak separation (Fig. 8b), and rainfall-adjusted storage anomaly (Fig. 8f) produced substantially larger variations in F1 score, with changes of 7.98, 4.11, and 3.64 percentage points, respectively. These results indicate that the framework is primarily sensitive to the temporal organization of continuous wetting responses and the discrimination of irrigation signals from rainfall inputs, rather than to any single anomaly-intensity threshold.

The relatively high sensitivity to the temporal parameters reflects the scale mismatch between continuous soil moisture responses and discrete irrigation records. Soil moisture time series characterize the hydrological response that develops and persists after irrigation inputs, whereas irrigation records describe discrete irrigation operations. A single water input may generate a wetting process lasting several days, while temporally proximate irrigation inputs may produce overlapping responses in the soil moisture time series. The candidate peak separation and the event merge gap therefore jointly determine how continuous wetting responses are identified and organized into discrete irrigation events. Both parameters exhibited pronounced asymmetric sensitivity curves: shortening the temporal scales caused relatively limited changes in detection performance, whereas excessive increases in the candidate peak separation or event merge gap led to clear declines in F1 score. Although broader temporal constraints can reduce duplicate responses generated by the same wetting process, they also increase the likelihood that temporally proximate independent irrigation events are merged, thereby reducing the one-to-one correspondence between detected events and reference irrigation records.

The rainfall-adjusted storage anomaly and the immediate storage response primarily influence the water-source attribution and temporal localization of anomalous wetting responses. The former determines whether an observed increase in soil water storage remains significantly positive after accounting for cumulative rainfall over the corresponding period, whereas the latter requires irrigation responses to exhibit a clear one-day wetting signal in 0–30 cm soil water storage. Both parameters maintained relatively high detection performance over intermediate ranges, indicating that water-source attribution requires an appropriate balance between excluding rainfall-dominated wetting responses and retaining irrigation events involving rainfall–irrigation overlap. The opposing changes in Precision and Recall associated with variations in the background recession percentile

https://doi.org/10.5194/egusphere-2026-6297
Preprint. Discussion started: 17 November 2026
© Author(s) 2026. CC BY 4.0 License.

suggest that this parameter mainly adjusts the detection scale used by the no-irrigation baseline to distinguish anomalous water inputs, rather than directly providing evidence of their water source.

The performance of irrigation event detection with parameter variations showed some site-specific differences (Fig. 8i). US-Ne2 was more sensitive to the candidate peak separation and the rainfall-adjusted storage anomaly, which may be related to the relatively high proportion of irrigation events overlapping with rainfall at this site. Under such conditions, wetting responses induced by individual irrigation events are more likely to overlap temporally with nearby irrigation inputs or rainfall. F1 was most sensitive to the event merge gap, which may be associated with the shorter intervals between neighboring irrigation events at this site. When multiple responses occur consecutively over a short period, changes in the consolidation scale can directly affect whether they are interpreted as a single persistent wetting process or as multiple independent irrigation events. In contrast, Daman remained relatively stable under most parameter perturbations, which may be related to its drier rainfall background and flood irrigation practice. Under these conditions, irrigation-induced wetting responses may be more pronounced relative to natural moisture variability.

Overall, the unified parameter settings exhibited good stability across the five sites. However, when extending the framework to new soil, climatic, and irrigation conditions, particular attention should be given to the parameters governing temporal consolidation and water-source attribution.

https://doi.org/10.5194/egusphere-2026-6297
Preprint. Discussion started: 17 November 2026
© Author(s) 2026. CC BY 4.0 License.

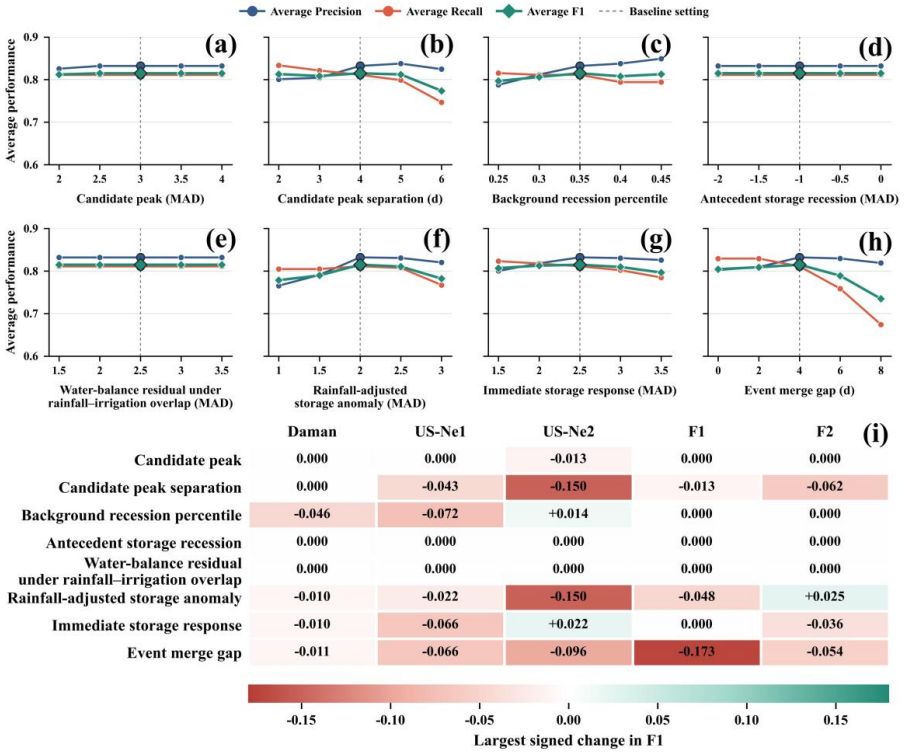


Fig. 8. Effects of eight key parameters on irrigation event detection performance. (a–h) Changes in the mean Precision, Recall, and F1 score across the five sites as candidate peak, candidate peak separation, background recession percentile, antecedent storage recession, water-balance residual under rainfall–irrigation overlap, rainfall-adjusted storage anomaly, immediate storage response, and event merge gap were varied, respectively; (i) site-specific F1 changes to perturbations in the different parameters.

4.2 Soil moisture response characteristics of matched and missed irrigation events

Fig. 9 illustrates the magnitude of soil moisture responses associated with matched and missed irrigation events relative to the site-specific background variability. At Daman, the standardized anomalies in 0–10 cm surface wetting (Fig. 9a), 0–30 cm soil water storage change (Fig. 9b), and cumulative water-balance residuals (Fig. 9c) were generally higher, indicating that most detected irrigation events produced pronounced soil moisture responses that deviated from the background variability at this site. The relatively broad distributions also indicate substantial variation among individual irrigation events in the magnitude of their departures from the background. In contrast,

https://doi.org/10.5194/egusphere-2026-6297
Preprint. Discussion started: 17 November 2026
© Author(s) 2026. CC BY 4.0 License.

the three standardized anomalies at US-Ne1 and US-Ne2 were more concentrated toward lower values, suggesting weaker contrast between irrigation-induced changes and routine soil moisture variability at these sites and a greater likelihood of overlap with background dynamics. F1 and F2 showed different response characteristics, F1 exhibited a relatively broad distribution of the three standardized anomalies, whereas F2 showed a more concentrated distribution with substantial overlap with US-Ne1 and US-Ne2 sites.

The standardized anomaly intensities of matched and missed irrigation events did not form a clear and consistent separation. At US-Ne1 and US-Ne2, where missed events were more frequent, the medians of all three standardized anomaly were lower for missed events than for matched events, but the distributions of the two groups still overlapped across all three metrics. Weaker anomalous responses provide more limited evidence of wetting and departure from background dynamics and are therefore more likely to result in missed detections. Daman, F1, and F2 had only 2, 1, and 3 missed events, respectively, and these few cases nevertheless exhibited different response characteristics. For example, the missed events at Daman still showed relatively high anomalies, whereas the missed event at F1 occurred within a relatively low response range. These results indicate that the degree to which an event scale soil moisture response stands out from the site-specific background is an important condition for irrigation event detectability, but not a sufficient condition for successful identification.

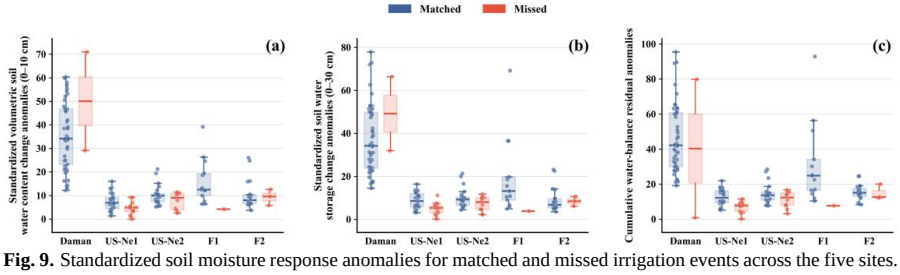


Fig. 9. Standardized soil moisture response anomalies for matched and missed irrigation events across the five sites. (a) Multi-timescale anomalies in mean volumetric soil water content over 0–10 cm; (b) multi-timescale anomalies in changes in 0–30 cm soil water storage; (c) cumulative water-balance residual anomalies over multiple temporal windows. Anomalies were standardized using the site- and metric-specific median and median absolute deviation (MAD); values are dimensionless.

https://doi.org/10.5194/egusphere-2026-6297
Preprint. Discussion started: 17 November 2026
© Author(s) 2026. CC BY 4.0 License.

4.3 Limitations of the study and prospects for future work

Although the proposed framework showed good consistency across different sites, crops, and irrigation methods , its applicability still needs to be further evaluated under a broader range of environmental conditions. Differences in soil properties, root-zone characteristics, irrigation regimes, and climatic backgrounds across regions may produce soil moisture response patterns that are not represented in the current samples. Future studies should conduct independent validation across a wider range of climate zones and agricultural systems, particularly through long-term observations in humid environments, during seasons with frequent or intense rainfall, and under different irrigation regimes, to further delineate the applicability and limitations of the method.

Second, this study relies on multi-depth ground-based soil moisture and rainfall observations, which can characterize irrigation responses and their vertical variability, but their observation scales differ substantially from those of satellite remote sensing. Satellite-based soil moisture products primarily represent surface conditions and are affected by vegetation cover, surface roughness, mixed-pixel effects, and retrieval errors. Future studies could integrate Sentinel-1, Sentinel-2, and other high-frequency soil moisture or land-surface state products to further evaluate the combined effects of temporal sampling, spatial scale, and observational uncertainty on irrigation event detection.

In addition, the effects of crop type and irrigation method on detection performance were not evaluated separately in this study. Among the current sites, crop type, irrigation method, climate, and sensor configuration do not vary independently, and differences in site-level performance therefore cannot be uniquely attributed to crop type or irrigation method. Future studies could conduct stratified evaluations using year-specific crop and irrigation management records and further distinguish the effects of management conditions from those of environmental background by establishing multi-field observations covering different crop–irrigation method combinations.

5 Conclusion

This study developed an irrigation event detection framework that integrates multi-timescale soil moisture dynamics and water-balance constraints. Validation against 149 reference irrigation events across five sites in China, the United States, and Morocco demonstrated that the framework

https://doi.org/10.5194/egusphere-2026-6297
Preprint. Discussion started: 17 November 2026
© Author(s) 2026. CC BY 4.0 License.

maintained relatively stable irrigation event detection performance under different climatic backgrounds and irrigation conditions, with mean Precision, Recall, and F1 scores of 0.832, 0.811, and 0.815, respectively, and site-level F1 scores ranging from 0.710 to 0.957. Compared with rain-free irrigation conditions, rainfall–irrigation overlap substantially increased the difficulty of irrigation event detection, although the framework still successfully identified most irrigation events under different rainfall conditions. Ablation analysis showed that direct soil moisture responses provided the primary observational basis for candidate event identification, while water-source attribution and soil water balance constraints helped distinguish water sources and identify changes deviating from the no-irrigation baseline, respectively. Auxiliary-depth responses mainly provided supplementary evidence for a subset of candidates. Missed irrigation events were jointly limited by weak or ambiguous wetting responses, temporal offsets between irrigation events and their soil moisture responses, and uncertainty in water-source attribution under rainfall conditions. As the observation interval increased, short-lived wetting responses and temporally proximate rainfall–irrigation processes were increasingly compressed into net changes between consecutive observations, with mean F1 scores declining to 0.62 and 0.53 at 5- and 6-day revisit intervals, respectively. Future work should incorporate actual satellite soil moisture observations and conduct validation under a broader range of hydroclimatic and agricultural management conditions to further assess the potential for regional-scale application. Overall, this study advances understanding of the temporal relationship between soil moisture responses and irrigation events and provides a methodological basis for extracting irrigation timing information from satellite soil moisture observations and extending event-scale irrigation monitoring to regional agricultural hydrology and water resources research.

CRediT authorship contribution statement

Shuaifeng Peng: Writing – original draft, Writing – review & editing, Methodology, Validation, Visualization, Data curation. **Jie Bai**: Writing – original draft, Writing – review & editing, Visualization. **Minghui Chang**: Writing – original draft, Visualization. **Jiayu Zhu**: Visualization, Data curation. **Guangcheng Shao**: Formal analysis, Data curation. **Linguang Miao**: Visualization, Data curation. **Jinrui Fan**: Visualization. **Shihua Li:** Funding acquisition, Project administration, Writing – original draft, Writing – review & editing, Conceptualization, Supervision.

https://doi.org/10.5194/egusphere-2026-6297
Preprint. Discussion started: 17 November 2026
© Author(s) 2026. CC BY 4.0 License.

Declaration of competing interest

The authors declare that they have no known competing financial interests or personal relationships that could have influenced the work reported in this paper.

Acknowledgments

This work was supported by the Sichuan Science and Technology Program under Grant 2026YFHZ0210

Data availability

The datasets for the Daman were obtained from the National Tibetan Plateau/Third Pole Environment Data Center (https://data.tpdc.ac.cn). The datasets for US-Ne1 and US-Ne2 are available through AmeriFlux (https://doi.org/10.17190/AMF/1246084 and https://doi.org/10.17190/AMF/1246085, respectively). The datasets for F1 and F2 are publicly available through the DataSuds repository (https://doi.org/10.23708/8D6WQC).

References

Amankwah, S.K., Ireson, A.M., Brannen, R., 2022. An improved model and field calibration technique for measuring liquid water content in unfrozen and frozen soils with dielectric probes. Vadose Zone Journal 21, e20225. https://doi.org/10.1002/vzj2.20225

Babaeian, E., Sadeghi, M., Jones, S.B., Montzka, C., Vereecken, H., Tuller, M., 2019. Ground, Proximal, and Satellite Remote Sensing of Soil Moisture. Reviews of Geophysics 57, 530–616. https://doi.org/10.1029/2018RG000618

Balenzano, A., Satalino, G., Lovergine, F.P., D'Addabbo, A., Palmisano, D., Grassi, R., Ozalp, O., Mattia, F., Nafría García, D., Paredes Gómez, V., 2022. Sentinel-1 and Sentinel-2 Data to Detect Irrigation Events: Riaza Irrigation District (Spain) Case Study. Water 14, 3046. https://doi.org/10.3390/w14193046

Bazzi, H., Baghdadi, N., Fayad, I., Zribi, M., Belhouchette, H., Demarez, V., 2020. Near Real-Time Irrigation Detection at Plot Scale Using Sentinel-1 Data. Remote Sensing 12, 1456. https://doi.org/10.3390/rs12091456

Brocca, L., Tarpanelli, A., Filippucci, P., Dorigo, W., Zaussinger, F., Gruber, A., Fernández-Prieto, D., 2018. How much water is used for irrigation? A new approach exploiting coarse

https://doi.org/10.5194/egusphere-2026-6297
Preprint. Discussion started: 17 November 2026
© Author(s) 2026. CC BY 4.0 License.



resolution satellite soil moisture products. International Journal of Applied Earth Observation and Geoinformation 73, 752–766. https://doi.org/10.1016/j.jag.2018.08.023

Chawla, I., Karthikeyan, L., Mishra, A.K., 2020. A review of remote sensing applications for water security: Quantity, quality, and extremes. Journal of Hydrology 585, 124826. https://doi.org/10.1016/j.jhydrol.2020.124826

Chen, Y., Lu, D., Luo, L., Pokhrel, Y., Deb, K., Huang, J., Ran, Y., 2018. Detecting irrigation extent, frequency, and timing in a heterogeneous arid agricultural region using MODIS time series, Landsat imagery, and ancillary data. Remote Sensing of Environment 204, 197–211. https://doi.org/10.1016/j.rse.2017.10.030

Gao, Y.-X., Leng, P., Li, J., Shang, G.-F., Zhang, X., Li, Z.-L., 2024. Identification of irrigation events using Bayesian statistics-based change detection and soil moisture measurements. Agricultural Water Management 302, 108999. https://doi.org/10.1016/j.agwat.2024.108999

González Perea, R., Camacho Poyato, E., Montesinos, P., Rodríguez Díaz, J.A., 2019. Prediction of irrigation event occurrence at farm level using optimal decision trees. Computers and Electronics in Agriculture 157, 173–180. https://doi.org/10.1016/j.compag.2018.12.043

Jalilvand, E., Kumar, S.V., Truong, C., Haacker, E., Mahanama, S., 2026. Characterization of irrigation timing using thermal satellite observations, a data-driven approach. Remote Sensing of Environment 333, 115153. https://doi.org/10.1016/j.rse.2025.115153

Jalilvand, E., Tajrishy, M., Ghazi Zadeh Hashemi, S.A., Brocca, L., 2019. Quantification of irrigation water using remote sensing of soil moisture in a semi-arid region. Remote Sensing of Environment 231, 111226. https://doi.org/10.1016/j.rse.2019.111226

Le Page, M., Jarlan, L., El Hajj, M.M., Zribi, M., Baghdadi, N., Boone, A., 2020. Potential for the Detection of Irrigation Events on Maize Plots Using Sentinel-1 Soil Moisture Products. Remote Sensing 12, 1621. https://doi.org/10.3390/rs12101621

Le Page, M., Nguyen, T., Zribi, M., Boone, A., Dari, J., Modanesi, S., Zappa, L., Ouaadi, N., Jarlan, L., 2023. Irrigation Timing Retrieval at the Plot Scale Using Surface Soil Moisture Derived from Sentinel Time Series in Europe. Remote Sensing 15, 1449. https://doi.org/10.3390/rs15051449

https://doi.org/10.5194/egusphere-2026-6297
Preprint. Discussion started: 17 November 2026
© Author(s) 2026. CC BY 4.0 License.



Liu, J., Hao, Z., Wang, J., Zhao, H., He, J., Xiao, Y., 2026. A Dynamic Irrigation Event Identification Method Driven by Spatiotemporal Fusion and Dynamic Samples Using an Attention-Enhanced Bi-LSTM Model. Remote Sensing 18, 2367. https://doi.org/10.3390/rs18142367

LIU, S., CHE, T., XU, Z., REN, Z., TAN, J., ZHANG, Y., 2025. Dataset of Heihe integrated observatory network (an observation system of Meteorological elements gradient of Daman Superstation, 2024). https://doi.org/10.11888/Terre.tpdc.302900

LIU, S., CHE, T., XU, Z., REN, Z., TAN, J., ZHANG, Y., 2024. Dataset of Heihe integrated observatory network (an observation system of Meteorological elements gradient of Daman Superstation, 2023). https://doi.org/10.11888/Terre.tpdc.301263

LIU, S., CHE, T., XU, Z., REN, Z., TAN, J., ZHANG, Y., LI, X., 2023. Dataset of Heihe integrated observatory network: an observation system of Meteorological elements gradient of Daman Superstation, 2022. https://doi.org/10.11888/Atmos.tpdc.300630

LIU, S., CHE, T., XU, Z., REN, Z., TAN, J., ZHANG, Y., LI, X., 2022. Qilian Mountains integrated observatory network: Dataset of Heihe integrated observatory network (an observation system of Meteorological elements gradient of Daman Superstation, 2021). https://doi.org/10.11888/Atmos.tpdc.272478

LIU, S., CHE, T., XU, Z., REN, Z., TAN, J., ZHANG, Y., LI, X., 2021. Qilian Mountains integrated observatory network: Dataset of Heihe integrated observatory network (an observation system of Meteorological elements gradient of Daman Superstation, 2020). https://doi.org/10.11888/Meteoro.tpdc.271414

LIU, S., CHE, T., XU, Z., REN, Z., TAN, J., ZHANG, Y., LI, X., 2020. Qilian Mountains integrated observatory network: Dataset of Heihe integrated observatory network (an observation system of Meteorological elements gradient of Daman Superstation, 2019). https://doi.org/10.11888/Meteoro.tpdc.270699

LIU, S., LI, X., CHE, T., XU, Z., REN, Z., TAN, J., 2019. Qilian Mountains integrated observatory network: Dataset of Heihe integrated observatory network (an observation system of meteorological elements gradient of Daman superstation, 2018). https://doi.org/10.11888/Meteoro.tpdc.270776

https://doi.org/10.5194/egusphere-2026-6297
Preprint. Discussion started: 17 November 2026
© Author(s) 2026. CC BY 4.0 License.



LIU, S., LI, X., CHE, T., XU, Z., REN, Z., TAN, J., 2018. HiWATER： Dataset of hydrometeorological observation network (an observation system of meteorological elements gradient of Daman Superstation, 2017). https://doi.org/10.3972/hiwater.15.2018.db

LIU, S., LI, X., CHE, T., XU, Z., REN, Z., TAN, J., 2015. HiWATER: Dataset of hydrometeorological observation network (an observation system of meteorological elements gradient of Daman Superstation, 2016). https://doi.org/10.3972/hiwater.455.2017.db

Muturi, J.W., Ndehedehe, C.E., Kennard, M.J., 2025. A review of the use of remote sensing techniques in assessing irrigation water use. Agricultural Water Management 319, 109759. https://doi.org/10.1016/j.agwat.2025.109759

Ouaadi, N., Ezzahar, J., Khabba, S., Er-Raki, S., Chakir, A., Ait Hssaine, B., Le Dantec, V., Rafi, Z., Beaumont, A., Kasbani, M., Jarlan, L., 2021. C-band radar data and in situ measurements for the monitoring of wheat crops in a semi-arid area (center of Morocco). Earth System Science Data 13, 3707–3731. https://doi.org/10.5194/essd-13-3707-2021

Ozdogan, M., Yang, Y., Allez, G., Cervantes, C., 2010. Remote Sensing of Irrigated Agriculture: Opportunities and Challenges. REMOTE SENSING 2, 2274–2304. https://doi.org/10.3390/rs2092274

Pereira, L.S., Paredes, P., Jovanovic, N., 2020. Soil water balance models for determining crop water and irrigation requirements and irrigation scheduling focusing on the FAO56 method and the dual Kc approach. Agricultural Water Management 241, 106357. https://doi.org/10.1016/j.agwat.2020.106357

Qian, X., Qi, H., Shang, S., Wan, H., Wang, R., 2022. Multi-year mapping of flood autumn irrigation extent and timing in harvested croplands of arid irrigation district. GIScience & Remote Sensing 59, 1598–1623. https://doi.org/10.1080/15481603.2022.2126342

Rousseeuw, P.J., Croux, C., 1993. Alternatives to the Median Absolute Deviation. Journal of the American Statistical Association 88, 1273–1283. https://doi.org/10.1080/01621459.1993.10476408

Suyker, A., 2016a. AmeriFlux US-Ne1 Mead - irrigated continuous maize site. https://doi.org/10.17190/AMF/1246084

https://doi.org/10.5194/egusphere-2026-6297
Preprint. Discussion started: 17 November 2026
© Author(s) 2026. CC BY 4.0 License.



Suyker, A., 2016b. AmeriFlux US-Ne2 Mead - irrigated maize-soybean rotation site. https://doi.org/10.17190/AMF/1246085

Xiang, Z., Moriasi, D.N., Samimi, M., Mirchi, A., Taghvaeian, S., Steiner, J.L., Verser, J.A., Starks, P.J., 2025. SWAT-IRR: A new irrigation algorithm for soil and water Assessment tool to facilitate water management and Conservation in irrigated regions. Computers and Electronics in Agriculture 232, 110142. https://doi.org/10.1016/j.compag.2025.110142

Yan, S., Liu, G., Dong, J., Wen, Z., Qiu, X., Li, D., 2026. Mapping winter irrigation areas and timing in arid regions using time series remote sensing data. Agricultural Water Management 326, 110154. https://doi.org/10.1016/j.agwat.2026.110154

Zappa, L., Dari, J., Modanesi, S., Quast, R., Brocca, L., De Lannoy, G., Massari, C., Quintana-Seguí, P., Barella-Ortiz, A., Dorigo, W., 2024. Benefits and pitfalls of irrigation timing and water amounts derived from satellite soil moisture. Agricultural Water Management 295, 108773. https://doi.org/10.1016/j.agwat.2024.108773

Zappa, L., Schlaffer, S., Brocca, L., Vreugdenhil, M., Nendel, C., Dorigo, W., 2022. How accurately can we retrieve irrigation timing and water amounts from (satellite) soil moisture? International Journal of Applied Earth Observation and Geoinformation 113, 102979. https://doi.org/10.1016/j.jag.2022.102979